Environmental Earth Sciences (2020) 79:318
https://doi.org/10.1007/s12665-020-09020-4

ORIGINAL ARTICLE

Material sources supplying debris flows in Jiangjia Gully

Tian Xiafei[1,3] · Su Fenghuan[1,2] · Guo Xiaojun[1,2] · Liu Jingjing[1,2,4] · Li Yong[1,2]

Received: 30 December 2018 / Accepted: 24 May 2020 / Published online: 25 June 2020

Abstract
Debris flow susceptibility is usually evaluated through material supplies and topographic features and the formation of debris flow is ascribed to the factors over the whole valley, almost ignoring detailed distribution of material sources and variety of behaviors in different tributaries. So far, there is not a comprehensive picture of debris flow developing from source tributaries to mainstream channel. Debris flow in Jiangjia Gully (JJG) exhibits diversity of surges and vivid scenarios concerning the forming and developing mechanisms. This study takes JJG as an example to explore how the materials are distributed in the valley and how the spatial heterogeneity of material distribution and tributary evolution influence the forming of variety of debris flow surges. It is found that most materials are distributed in tributaries of active stages with evolution index between 0.55 and 0.65; the occurrence of debris flow relies more on the spatial distribution of source tributaries than on the quantity of the material. Local conditions of tributaries, such as the concentration of materials, the granular structure of soils, and the locations receiving frequent rainfalls, are the very factors governing a debris flow event. It is the spatial heterogeneity of sources and material supplies that result in the variety of debris flow surges in JJG. Similar mode is believed to occur in debris flows in other regions.

Keywords Landslide distribution · Tributary evolution · Debris flow surge formation · Rainfall · Probability distribution

Introduction

Debris flow prediction and assessment rely on understanding of material sources and topography over the whole valley (Lorente et al. 2003; Tunusluoglu et al. 2008; Dong et al. 2009; Kappes et al. 2011; Qiao et al. 2012). Remote sensing images and Geographic Information System (GIS) techniques make it possible to obtain material distribution and related topographic data (Rickenmann 1999; Chen and Lee 2000; Fannin and Wise 2001; Crowley et al. 2003; Rickenmann et al. 2006; Blahut et al., 2010; Garcia-Davalillo et al. 2014; Gonzalez-Diez et al. 2014; Iverson 2014; Nakata and Matsushima 2014; Royan et al. 2014). The quantity of materials is usually considered as the major factor and attention has been mainly paid to the mapped distribution of source areas, almost ignoring the difference in material behaviors and the variety of effects due to spatial distributions of materials (Shieh et al. 1996; Iverson and George 2016). For example, materials receiving less rainfall or located in gentle slopes are not so active as those receiving heavy rainfall and in steep slopes. Moreover, materials are in various physical and mechanical conditions and contribute to debris flows in different manners. Materials in stream channels are dominated sources for debris flows in burned areas (Santi et al. 2008); while for other cases, slope failures and landslides are the main sources. The spatial distribution of materials and their quantities do not suffice to evaluate the potential of debris flows, let alone predict the occurrence. There are so many cases that a valley is abundant of loose materials that are believed to be potential supplies but has only occurrences at very low frequency (e.g., once in more than ten years). Only when materials are considered in association with the processes of specific event, we can really identify the sources of debris flows.

✉ Su Fenghuan
fhsu@imde.ac.cn

1 Key Laboratory of Mountain Hazards and Surface Process, Chinese Academy of Sciences, Chengdu 610041, China

2 Institute of Mountain Hazards and Environment, Chinese Academy of Sciences, Chengdu 610041, China

3 University of Chinese Academy of Sciences, Beijing 100081, China

4 State Key Laboratory of Hydraulics and Mountain River Engineering, Sichuan University, Chengdu 610065, China

Living debris flows are rarely witnessed in field and it is even harder to trace where and how the source materials take actions. Jiangjia Gully (JJG) has provided an ideal place for debris flow monitoring, where each year sees on average a dozen of occurrences, with each consisting of tens or even hundreds of flow surges in various regimes and magnitudes, and a long-term observation dataset of more than 6000 surges is available in the Observation Station of JJG (Li and Luo 1981; Li et al. 1983; Davies et al. 1991, 1992; Li et al. 2004; Liu et al. 2009; Li et al. 2012, 2013). Surge phenomenon implies that debris flow does not depend on the full-valley factors such as the total drainage area, the average slope, and the mainstream length; on the contrary, each debris flow event originates from special sources under favorable local material and rainfall conditions. As indicated by the high variety in material compositions, the surges within a debris flow event cannot come from a single source and in a unique forming and evolving process. The surges in various appearances indeed hint at their sources and originations. Therefore, it is possible to use the surge data in JJG to associate surges with special sources and further explore the real sources of high potentiality. The present study provides the material distributions in tributaries and their relations to debris flow development. As surge phenomenon is ubiquitous over the world (e.g., Rickmers 1927; Blackwelder 1928; Sharp 1942, 1953; Broscoe and Thompson 1969; Pierson 1980, 1986; Takahashi 1991, 2007; Major 1997; Arattano and Marchi 2000), the study in JJG is also helpful and heuristic for understanding debris flows in other regions.

Materials and methods

Physical background and data sources

Outline of the study area

The major materials for the study include the physical background of debris flows in JJG, especially the tributary features and their material supplies to debris flows, and the observation data of debris flow surges.

The JJG lies in the east bank of the Xiaojiang River, a tributary of the Upper Yangtze, in the northeast Yunnan plateau. It is 48.6 km^2 in area, with a mainstream length of 13.9 km. The valley extends along the seismic faults and frequent earthquakes make the rocks fragile and easily weathered. The outcrops are dominated by pre-Cambrian epimetamorphic rocks, such as slate, phyllite, and shale, all being easily weathered to form fragmental clastics. Accordingly, quaternary diluvium and colluvium are widely distributed in slopes, occupying 80% of the valley area, providing abundant material supplies to debris flows.

Geomorphologically, JJG has a great relief with elevation difference of 2229 m, from the top at 3269 m down westwards in steps to the junction into Xiaojiang at 1040 m. The slope is 43° on average and 88° at the extreme. Slopes between 30° and 70° occupy 68% of the total area, which are highly potential to landslides and soil failures because the slope is much higher than the friction angle. The gradient of stream channels in the upper reaches is 25% on average and 35% or more in some sections, with cascaded water falls up to 4–6 m in the channel. Moreover, the gourd-ladle shape of the drainage basin is well favorable for the collection of water and material restoration, since both material sources and rainfalls are concentrated in the upper reaches of JJG, contributing to the "gourd". Besides, there are more than 200 major tributaries, with stream channel density of 2.56–3.2 per km (Fig. 1). All these are facilitating the accumulation of water and materials, and acceleration and incision of mass movement, providing favorable conditions for debris flows.

There are several major gullies contributing to the mainstream: the Menqian Gully, Duozhao Gully, Dawazi Gully, Chaqing Gully, and Laojiangjia Gully, among which the most active is the Menqian (Fig. 1). Field survey indicates that Menqian has 65 major tributaries (bigger than 0.1 km^2) in fan shape; while the Duozhao has 76 dendritic tributaries (as eye-identified in the map of 1:50,000). Besides, there are still more than 100 small gullies (much smaller than 0.1 km^2) and numerous drills in the upper reaches, cutting the slopes into fragmented pieces to become scattering sources for debris flows. It is found that a debris flow does not come from some single tributary, but from different tributaries; and some tributaries are active, while others are not so active alike. For example, in the last decades, almost all debris flows came from Menqian and few from Duozhao. This spatial heterogeneity plays a crucial role in developing debris flows, which is well represented by the appearances of surge waves.

Debris flow surges in JJG

Debris flows in JJG move in manner of surge waves; each event consists of tens or hundreds of surges with different debris compositions and flow properties. For example, a single debris flow event occurred on July 9, 1991(event 910,709), which started at 4:10:00 in the morning and ended at about 19:30:00 in the evening, delivering more than 1.6×10^6 m^3 of sediment. During the period, there were 427 surges coming in succession, with time interval of 125 s on average. These surges fluctuated considerably, with discharge (Q) fluctuating from 1.4 to 680 m^3/s, density (ρ) from 1.3 to 2.25 g/cm^3, and velocity (v) from 2.5 to 11.1 m/s. Figure 2 shows the parameter variations on average for several surge groups as circled in the plot.

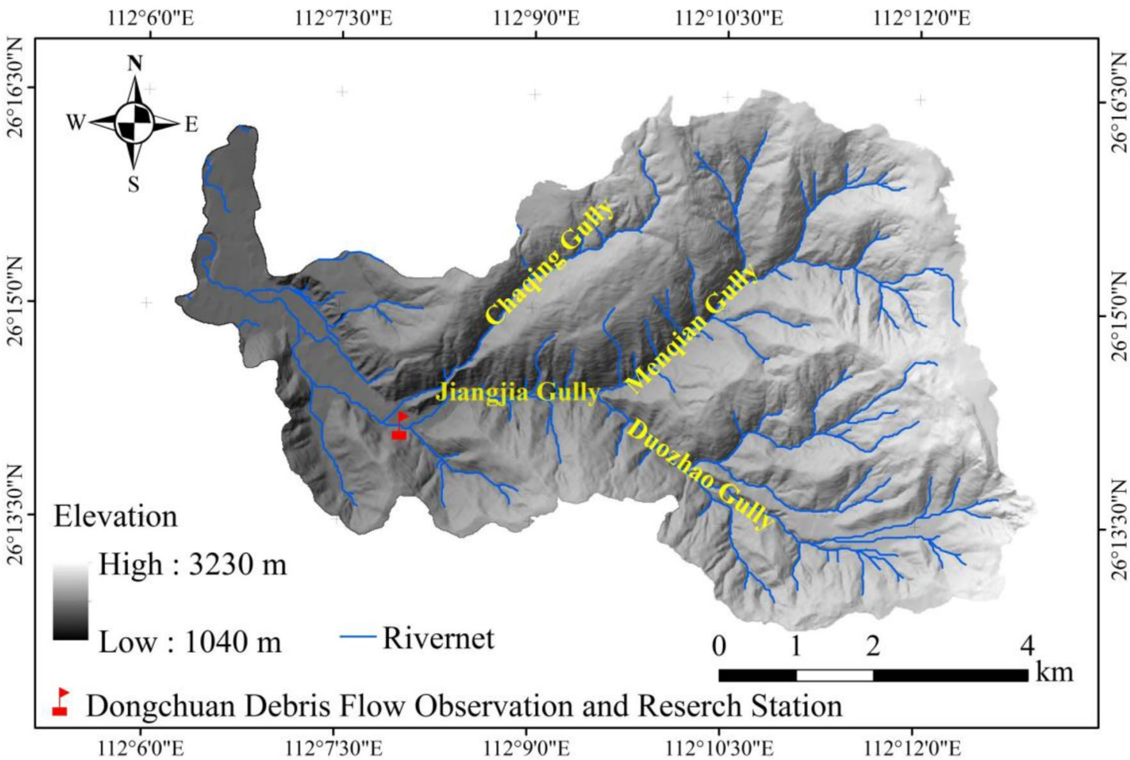

Fig. 1 Basic background condition of JJG

Fig. 2 Hydrographs of debris flow event 910,709

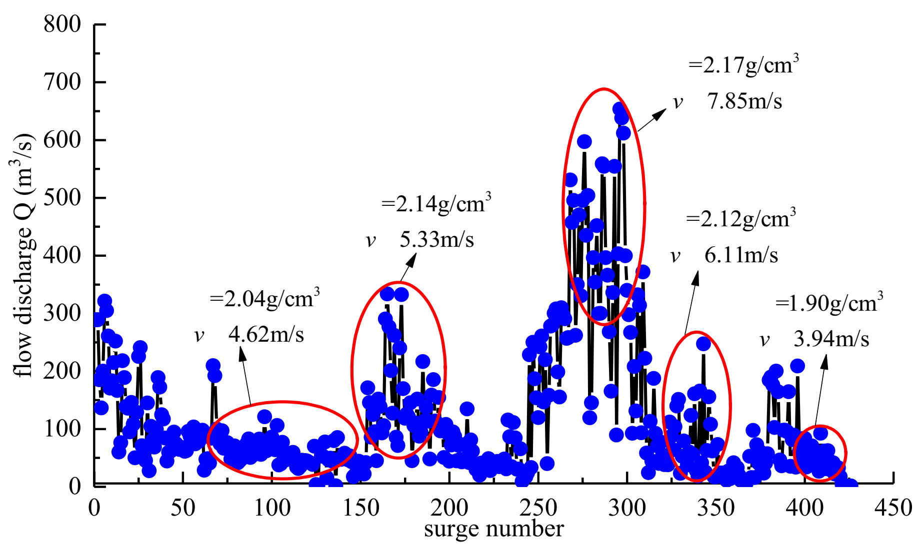

It is noted that flows with density below 1.5 g/cm^3 are not really debris flow but hyperconcentrated flows. This means that debris flows do not coincide with water flood, which further implies that soil materials do not always supply water flows. In other words, the soils and water are transported through separated processes. Debris flow occurs only when the two components are coincided in space and time. Moreover, the variation of flow density corresponds to change in material composition, implying that the materials are supplied from different sources. The Station of Observation and Research of Debris flows of the Academy of Sciences of China has monitored debris flows in JJG since 1960s and achieved a dataset of including more than 6000 surges (Cui et al. 2005; Li et al. 2009), based on which it is found that a surge formation involves water process and soil process. As water process is the major concern for hydrology, the present study considers mainly the soil process, i.e., the material supplies to debris flow surges. Therefore, the focus is to determine the material sources and their activities in different tributaries, which finally determine how source materials supply to surges.

Methods and data processing

Interpretation of material sources

The purpose of the study is to associate the surges to the possible material sources, then the major methods are in terms of GIS and remote sensing interpretation, combining with field surveys and statistic analysis.

Material sources for debris flows in JJG are mainly of loose deposits of shallow slope failures and sediments of old debris flows in channels. As shown in Fig. 3, the photos a, b, c, d represent four typical situations of materials in the tributaries, indicating different types of loose materials in channels and slopes.

For identifying these sources over the whole valley, Quickbird image of 0.61-m resolution is used, with radiation and geometry correction. In operation, the spectrum bands B4, B3, B2, with geometric rectification and Band PAN, are applied to false color image, and the material blocks are easily identified as polygons in different features of tone, texture, pattern and shape. The high resolution of the images ensures the reliability of the identification of material source blocks in various sizes. A total of 906 material blocks have been identified in different tributaries, with areas ranging from 0.38 m^2 to 6.7×10^5 m^2, amounting to 15.30 km^2. The material blocks include landslides, soil failures, debris flows, and potential active mass deposits on slopes.

Hypsometric analysis and evolution division of tributaries

Almost all sources are located in tributaries, then various tributaries are necessarily identified to find their relationship with the sources. A tributary is easily abstracted from DEM (digital elevation model), which can be automatically realized under GIS tools generating water system through modeling surface run-off flow. For the present, 550 tributaries, covering 46.1 km^2, about 95% of the total valley, are taken

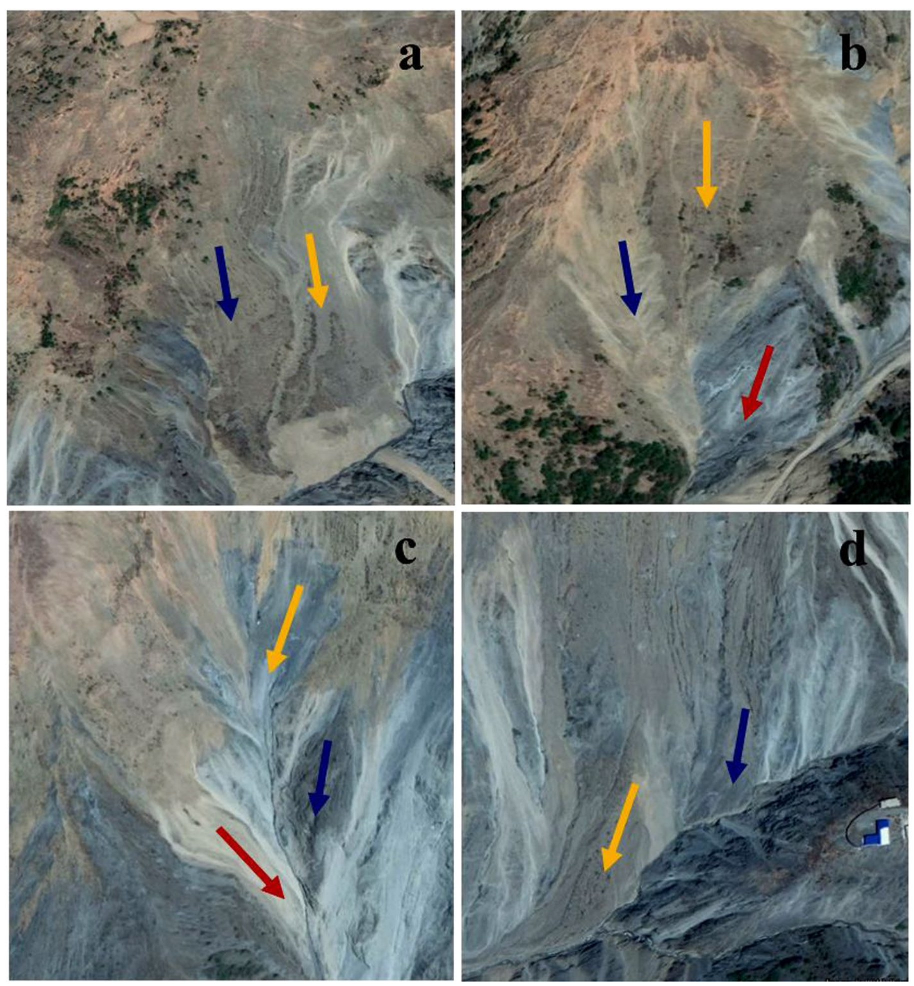

Fig. 3 Different types of material sources

from the 1:10 000 DEM of JJG, using hydrology analysis module in ArcGIS 10.2 software spatial analysis function.

Hypsometric analysis is employed to describe a tributary by the hypsometric curve (*H*-curve), which is also known as the area-elevation curve, defined as an area function varying with elevation (Strahler 1952, 1957). The H-curve expresses the elevation (rescaled as *h/H*, with *h* the elevation relative to the outlet point of the tributary and *H* the maximal elevation) as function of drainage area at the given point (rescaled as *a*/*A*, with *a* the area at the point and *A* the total area of the tributary). Formally, *H*-curve is expressed by

$$h/H = f(a/A), \quad (1)$$

or $h = f(a)$ when the coordinates of elevation and area are normalized. Simply speaking, *H*-curve tells how the drainage area varies with the elevation. Figure 3 shows some *H*-curves for some tributaries. In this study, the contour interval (i.e., the elevation difference between two neighboring contours) is 10 m, ensuring the accuracy of the resulting *H*-curves (Fig. 4).

According to the generation of *H*-curve, the area under the curve in the plot, or the integral of *H*-curve, represents the residual mass fraction in the tributary. For example, when the area is 1/3, it means that 2/3 of the tributary mass has already been eroded. Thus, the *H*-curve integral features the evolution of tributary and can be properly defined as the evolution index (EI), which is formally calculated as

$$\mathrm{EI} = \int_0^1 f(a)\mathrm{d}a. \quad (2)$$

In practice, the specific function *f*(*a*) is unnecessary; the integral can be simply obtained through figuring out the area in the plot. Obviously, large EI means a tributary in youth stage having large fraction of mass and, hence, more material for mass movement.

The interpretation of material sources and the corresponding tributaries provide the background basis for further exploration of debris flow sources.

Besides, the scaling distribution of grain size (Li et al. 2013) is used to feature the soil properties and active potential of the source materials.

Results and analysis

Material quantities over the valley

Based on field surveys, it is found that material sources of debris flows are widely distributed in JJG over the whole valley, in volume from potential landslides of about 1.23×10^9 m^3 (Du et al. 1987; Tian 1987; Wu et al. 1990), and from deposits in stream channels of about 7.5×10^8 m^3 (Yang 1997). Moreover, the surveys have indicated that there is a great difference between the two major branches of JJG, the north Menqian Gully and the south Duozhao Gully. Majority of slope sources and about 60% of debris flow deposits are

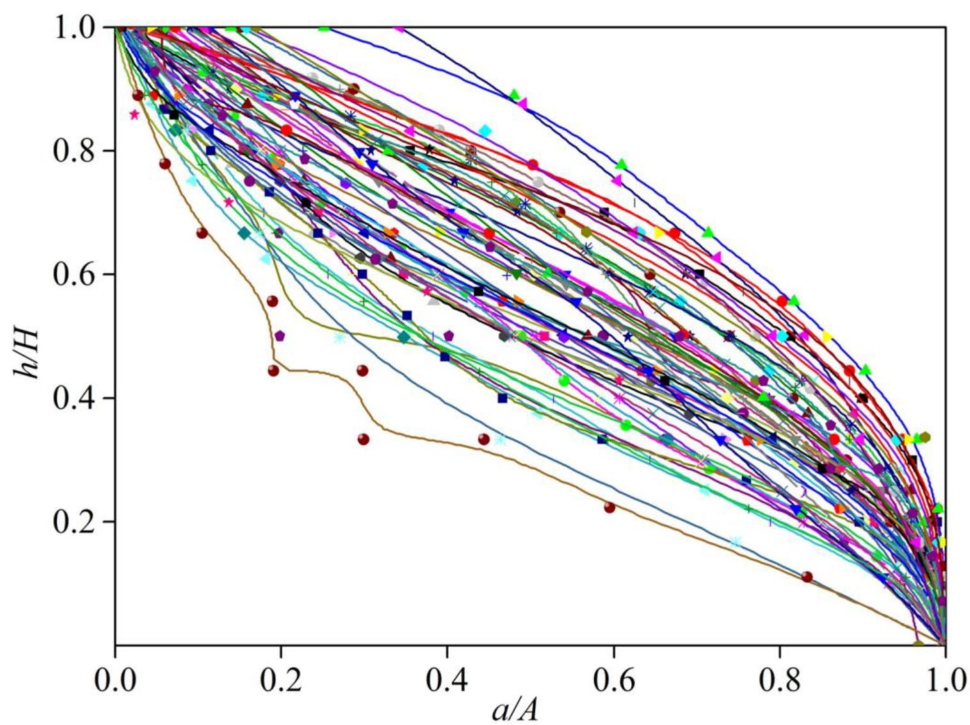

Fig. 4 Hypsometric curves of tributaries in JJG

located in Menqian. In fact, most all debris flows in the last decades come from Menqian areas.

Furthermore, the Quickbird image interpretation provides more accurate estimation of loose materials in specific major tributaries of the two branches, as listed in Table 1. Compared with the previous estimation, the quantities are less because they are derived directly from the "present" active landslides, excluding quantities from potential or historical landslides.

In these surveys, the landslide volume is calculated by the production of landslide area interpreted from the Quickbird image and the thickness estimated by the following empirical formula (Tian 1987):

$$d = (K \tan\theta + m)b, \tag{3}$$

where θ and b are average slope and width of the landslide. For $\theta \leq 45°$, $K = 0.225$ and $m = -0.041$.

However, these estimations are only helpful for evaluating the potentiality of debris flows at the valley scale, they tell little about the real sources for debris flow events. Difference between Menqian and Duozhao implies that even the gullies having large quantity of materials may not be the sources for debris flows. In fact, what are really associated with debris flow occurrence involve the following three problems: Where are the materials distributed? How are about their local conditions? What are their physical and mechanical properties? Incorporating all these issues in material supplying processes is the only way to understand the formation and evolution of debris flow. For the present purpose, the point at issue is the real sources where debris flows originate, then it is necessary to look the valley into even smaller scales, down to specific tributaries that directly provide material supplies for debris flows.

Material distribution in tributaries

Based on hypsometric analysis, the EI (Eq. 2) for each tributary is obtained, which is 0.508 on average, ranging between 0.32 and 0.84, with standard variance of $\sigma = 0.138$. Following the EI values, the tributaries are classified into five groups:

$$\begin{aligned} &\text{I } (< 0.35),\ \text{II } (0.35 - 0.45), \text{III } (0.45 - 0.55), \\ &\quad \text{IV } (0.55 - 0.65),\ \text{V } (> 0.65). \end{aligned} \tag{4}$$

Table 2 lists the EI divisions and corresponding material distribution, showing that materials are concentrated on tributaries with EI between 0.55 and 0.65.

Figure 5 has combined the EI division and material interpretation, showing the distribution of materials in tributaries. The materials in blue are overlapped with the freshcolor blocks, meaning that the overwhelming majority of materials are coincided with the young tributaries.

Table 1 Loose material quantities in tributaries of Menqian and Duozhao Gully

Branches	Tributaries	Landslides	Minimum (10^4 m^3)	Maximum (10^4 m^3)	Total (10^6 m^3)
Menqian	Sanjiacun	30	0.17	90.6	22.4
	Mashanao	30	0.56	885.5	34.2
	Dadi	18	0.91	868.6	49.3
	Mainstream	18	40.06	7004.0 (group)	222
	Total	96			328
Duozhao	Meizishu	26	0.11	604.07	25.8
	Xiazhuqing	6	1.64	330.92	7.8
	Daxiaoduozhao	18			2.1
	Mainstream	9	26.91	1682.97	58.7
	Total	59			94

Table 2 EI division and landslide/debris flow distribution

EI	Area (km^2)	Area fraction (%)	Landslide/debris flow area (10^4 m^2)	Fraction of total debris flow area (%)
I (<0.35)	0.00045	0.00	0	0
II (0.35–0.45)	0.77	1.58	8.77	0.57
III (0.45–0.55)	3.97	8.17	82.79	5.42
IV (0.55–0.65)	35.76	71.52	1295.82	84.86
V (>0.65)	6.62	13.62	139.15	9.11

Fig. 5 Material distribution at different EI division in JJG

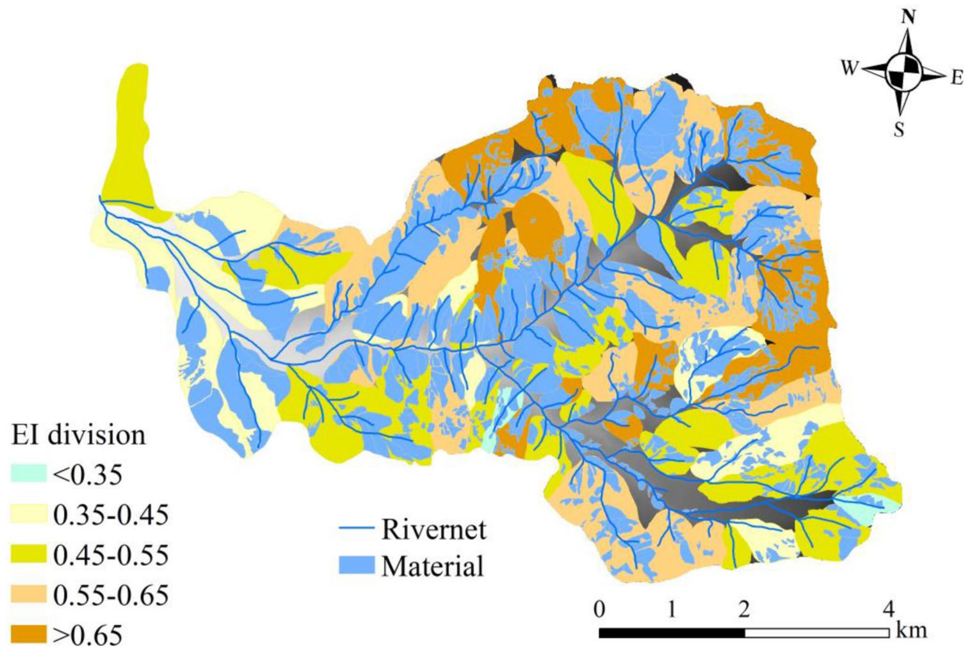

It is noted that the "old tributaries" (i.e., EI < 0.35 in shallow blue) are scattering along some big tributary channels; while, the young tributaries (EI > 0.65 m in dense brown) are scattering in boundary of the watershed, mainly around the north and east divide. More remarkable are concentrations of several "fleshcolor blocks", which are tributaries with EI between 0.55 and 0.65; and some scattering "yellow blocks", which are tributaries with EI between 0.45 and 0.55. In particular, the freshcolor blocks are mainly distributed in Menqian and along the mainstream channel of JJG; while in Duozhao, those tributaries are only in the south part at the middle stream. This clearly represents the difference of material sources in the two branches (cf. Table 1).

Figure 5 indicates that material distribution is non-uniform and majority is concentrated in the tributaries of high EI values (between 0.55 and 0.65); this exemplifies the spatial heterogeneity of material sources, which in turn determines the diverse activities of mass movements in tributaries. Roughly speaking, the tributaries with high material concentration are expected to be highly potential to debris flows.

Moreover, the EI is found to satisfy the Weibull distribution:

$$f(\beta) = \mathrm{Weib}(\beta;\lambda,k) = \frac{\lambda}{k}\left(\frac{\beta}{\lambda}\right)^{k-1}\exp(-(\beta/\lambda)^k), \quad (5)$$

where β is the EI value; λ and k are, respectively, the scale and shape parameter. For the present case, $\lambda = 0.53$ and $k = 11.73$, meaning that the EI on average is $0.53\Gamma(1 + 1/11.73) \sim 0.50$, with $\Gamma(x)$ being the Gamma function. The probability distribution provides an overall description of evolution state of a valley. With such a distribution function, comparisons between valleys can be made through the shape and scale parameters. In general, the higher the scale parameter, the younger the valley, and the higher the potential of valley activity.

The following discussion focuses on the details of existing and potential material sources in relation to various geomorphology elements and down to specific tributaries with different evolution state, geometric shape, and water system structure, so as to illustrate how the materials in different situations evolve and supply to debris flows.

Material distribution in relation to geomorphology elements

Material distribution with elevation

Elevation is usually considered as a factor deciding the gravity potential energy of the material. Figure 6 shows the materials distributed at different elevations. It is noted that the distribution presents little difference, except for the lowest and highest zones (Fig. 7). This means that the surface processes responsible for the materials are active at all elevations, responding to the fact that the rocks are fragile and intensively weathered, making slopes abundant of fractured debris.

In fact, the potential energy depends on the difference of elevation between the site of material and the end point of the mass movement. In this meaning, the elevation of material provides only a rough index for the potential. As materials considered here are distributed in specific tributaries, the

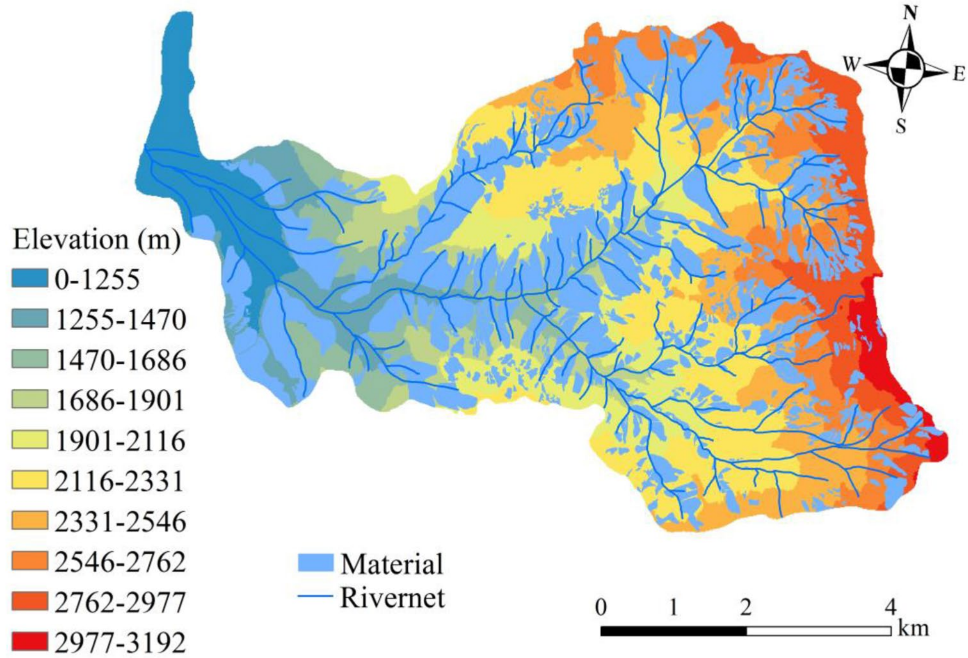

Fig. 6 Material distribution at different elevations

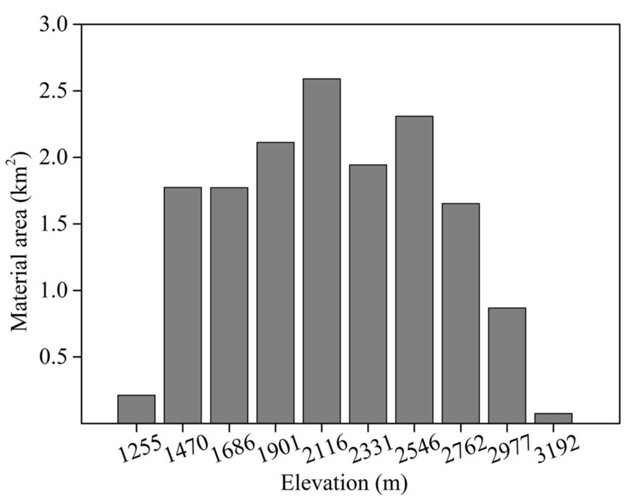

Fig. 7 Materials at different elevations

more direct controlling factor is the slope of the tributary, as discussed in the following.

Materials in tributaries of different slopes

As an overall indicator of relative relief, slope of a tributary is the average gradient of the stream, defined as $J = \Delta H/L$, where ΔH is the elevation difference between the top and outlet of the tributary and L is the streamlength of the channel. As shown in Figs. 8 and 9, materials are mainly distributed in tributaries with $J = 0.58$–1.19 (i.e., between 30 and 50°), and more than 31.26% (4.78 km^2) are bigger than 40° ($J = 0.84$). As J decreases with drainage area in a power law (Li et al. 2009), the high value of J means that the materials are mainly in small tributaries. And the high J also provides a possibility of long runout distance for landslides.

Gravity potential energy of a material block is determined by the relative elevation between its location and the outlet of the tributary, which can be roughly taken as a fraction of the overall relief of the tributary, $\alpha\Delta H = \alpha JL$. Thus, the potential energy P is evaluated as:

$$P = aMg\Delta H = aMgJL, \tag{6}$$

where M is the block mass, A is the drainage area of the tributary, g is the gravity acceleration, and α is a coefficient depending on the location of the mass, with $\alpha = 1$ when the mass block lies at the top. It is noted that this α is just the normalized elevation in the H-curve.

Since both L and J are related to the drainage area of the tributary through the Hack's law, $L \sim A^m$, and $J \sim A^{-k}$, Eq. 6 yields:

$$P = aMgA^{m-k}. \tag{7}$$

In general, $m = 0.57$ but for small tributaries m is about 0.50, and k is 0.20 on average (Li et al. 2009). This implies $P \sim A^{0.3}$, meaning that the potential increases with drainage area of the tributary. Equation 7 is meaningful here because both α and A are associated with H-curve and in principle, it is possible to find the distribution of α over a valley and, thus, the total potential can be evaluated.

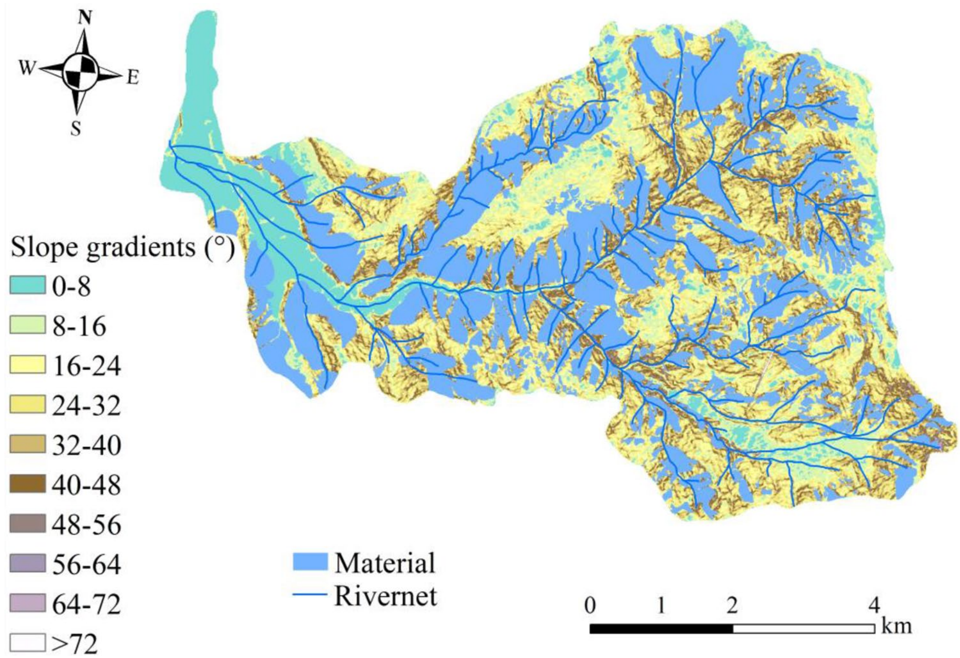

Fig. 8 Slope gradients of materials

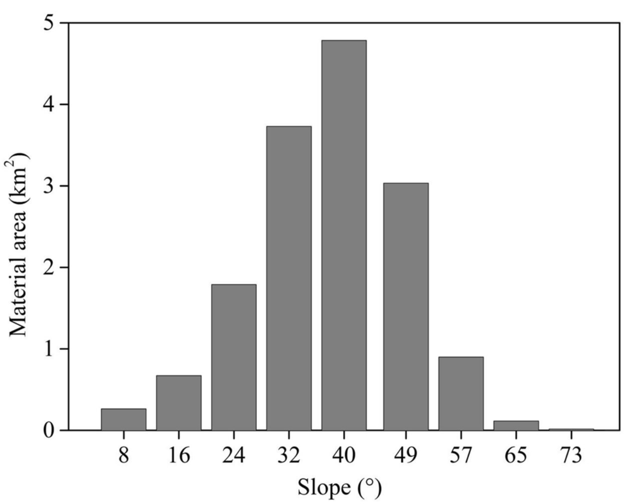

Fig. 9 Materials at different slopes

Material distribution with respect to aspect

Aspect responds to the receiving quantities of sunshine and rainfall, which are related to the moisture states and hydrological conditions, and thus of significance to the mass movements of the materials. But as shown in Figs. 10 and 11, the material distribution presents little difference in aspect, implying that the sources are governed mainly by the geological agents rather than the environmental (i.e., weather) influences. However, as slopes of different dip directions are under different conditions of precipitation, vegetation, the hydrology processes should be different, and thus, the materials at different aspects are believed to undergo different surface processes.

Material types and soil properties

Landslides types

Above discussions consider the spatial distribution of materials in blocks, ignoring types of materials. In fact, the material blocks consist of different types of materials connected in a tributary, such as landslide on slope or from talus, or colluviums. This can be illustrated by the Dadi gully, a tributary of Menqian. The Quickbird image clearly shows the landslides distribution (Fig. 12, in which the numbers are the codes of tributaries), from which the volumes of the landslides can be calculated through thickness estimation using Eq. 1; the results are listed in Table 3, showing that the majority of landslides occurs on the talus, accounting for about 70% of the total landslides area (or volume), and only about 30% occur on the slope. This means that the gully has been long fragile and slopes are "pre-deposited" by talus materials prone to failure. A remarkable feature is that almost all the slopes are near and bigger than 40°, which goes beyond the usual internal friction angle (about 25°–30°). Obviously, similar situations occur in many other tributaries, meaning that even a block of material may fall into different pieces of different potentiality to failure.

Fig. 10 Aspects of materials

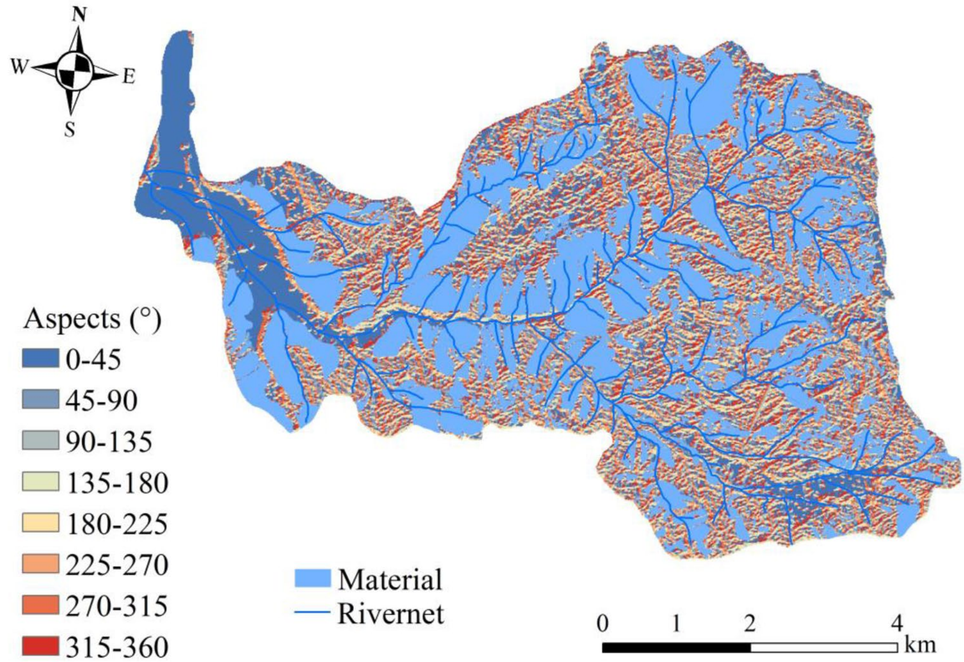

Slope of the materials

Materials are always in different slopes. Figure 13 shows several tributaries (e.g., No. 9, 10, 36, 47. 59, which are serial number of tributaries used for tributaries division), where the material blocks are divided into different slopes, ranging from 14° to 45° and mainly between 30° and 40°. The material slope is a crucial factor controlling landslides and soil failures. It is noted that the material slope is sometimes smaller than the tributary gradient; this is because the sources are distributed in the lower reaches of tributaries, which makes it easy for the materials to find ways into the channel.

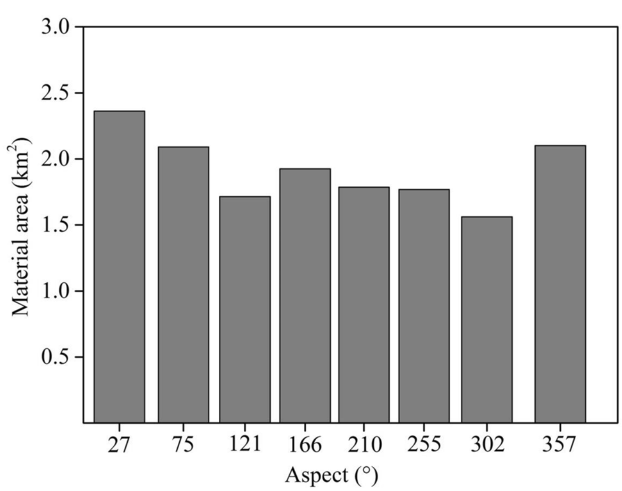

Fig. 11 Materials at different aspects

For example, consider a tributary by the mainstream of JJG, the Dawazi Gully, which is in area of 2.33 km^2 and stream length of 600 m. The materials are mainly on slope of 35°–45°, higher than the average repose angle and, thus, of high potentiality to slope failure (Table 4). Moreover, the materials are concentrated in the mid-lower reach, only 300 m to the junction; thus, the failures are easy to move downwards into the mainstream channel. In fact, debris flow occurred several times one year in this single gully (Chen et al. 2001).

The case of Dawazi indicates that the location of material in a tributary is also crucial for its contributing to debris flows. The location plays multi-roles of influence. Generally, material at high elevation usually has high gravity potential energy. But for a specific block of material, the gravity potential energy is determined by its height above the slope root but not the outlet of valley; therefore, the location on slope is of even more influence than the general elevation.

Two other tributaries are taken for comparison: one is taken from the Menqian (Fig. 14a) and the other from the lower reach of the mainstream of JJG (Fig. 14b). Numbers in the figures are also serial number of the tributaries as in Fig. 13. Material blocks in different slope gradient are denoted by different colors. In tributary A, material blocks with slope bigger than 40° are located on both banks of the lower reach and in B, they are in the upper reach. In case A, when slope failures occur, they easily find a way out to enter the mainstream channel; while in case B, the failures must take a long way to get out of the channel. Obviously, materials on the lower slopes are more potential to debris flows, given the same background.

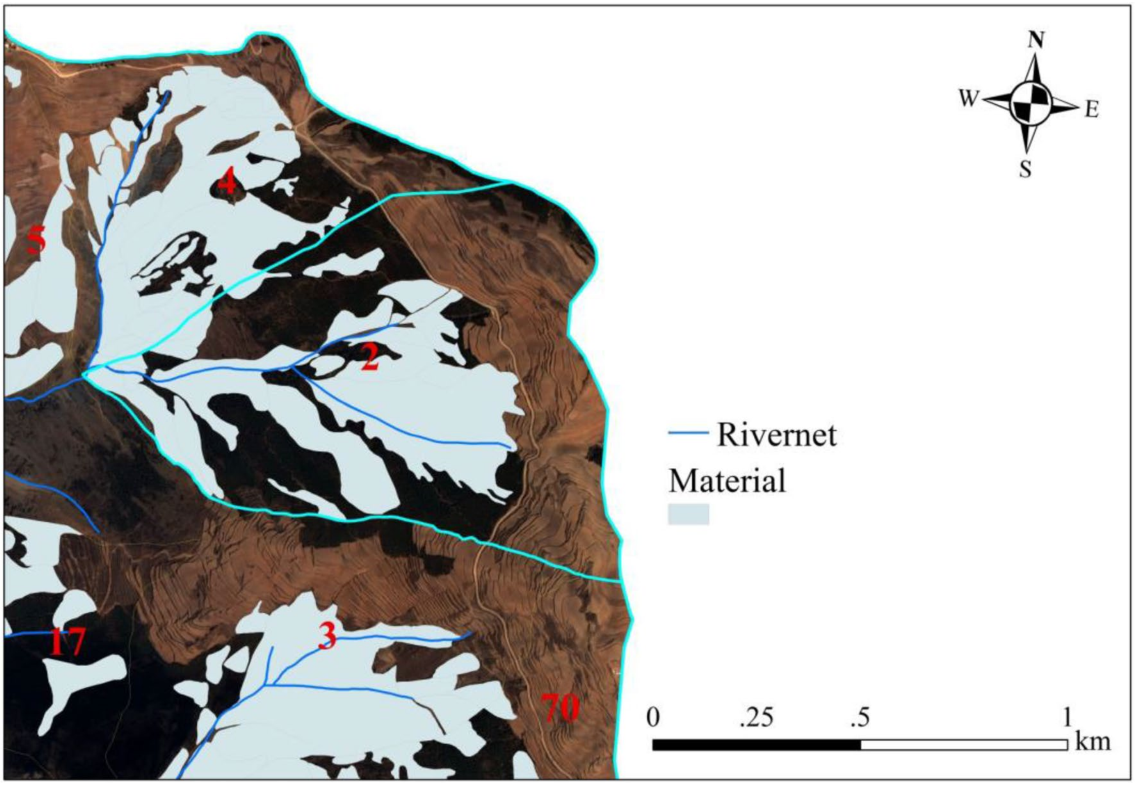

Fig. 12 Landslides distribution in tributary Dadi

Discussions above illustrate that for a specific material source, the material type, the slope, and the location are all influential for the mass movement and the potentiality to debris flows. It follows that materials should be assigned different potential to slope and channel process, depending on their specific situation in the valley.

Table 3 Landslides in tributary Dadi

No.	Landslide types	Width (m)	Slope (°)	Area (m^2)	*K*	Volume (10^4 m^3)
1	Talus	311.79	39.80	56,143.90	0.1463	256.10
2	Talus	416.03	42.70	113,727.10	0.1669	789.67
3	Talus	124.59	45.40	6980.78	0.1992	17.33
4	Talus	194.03	39.30	7712.78	0.1435	21.47
5	Talus	40.21	47.30	1191.14	0.1901	0.91
6	Talus	42.86	44.10	1482.53	0.1773	1.13
7	Talus	155.06	39.90	9521.32	0.1471	21.72
8	Talus	239.75	41.00	30,417.06	0.1547	112.81
9	Talus	387.63	39.20	97,087.26	0.1423	535.53
10	Slope	184.64	41.30	18,711.77	0.1570	54.24
11	Slope	74.58	36.60	6442.60	0.1262	6.06
12	Talus	54.44	42.30	13,641.10	0.1640	12.18
13	Slope	282.42	44.10	49,401.38	0.1768	246.67
14	Talus	483.79	42.80	107,259.11	0.1674	868.65
15	Slope	561.05	38.90	83,298.17	0.1407	657.55
16	Talus	323.29	39.90	42,915.23	0.1472	204.23
17	Talus	302.51	37.80	95,843.86	0.1334	386.78
18	Slope	450.85	41.10	104,557.86	0.1556	733.50

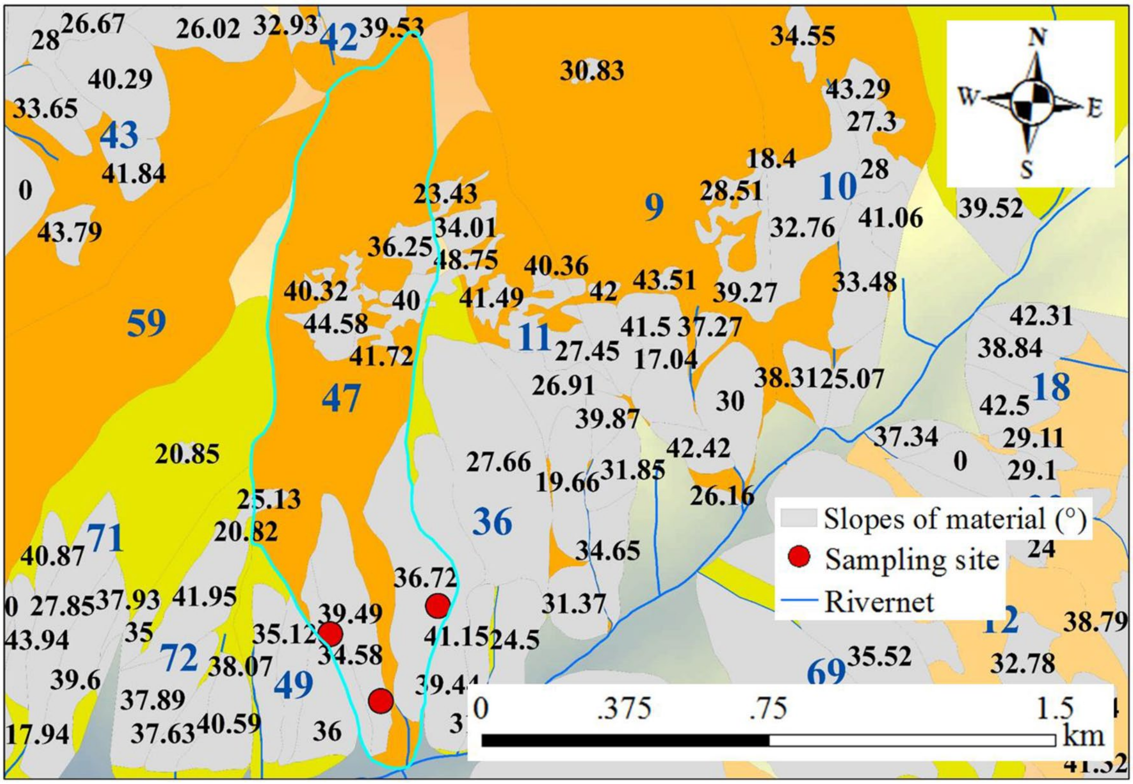

Fig. 13 Slopes of material blocks

Properties of materials

Besides the spatial distribution and local conditions, the soil structure of material is even more significant in influence. The soil features are described in term of grain composition, which is the fundamental property related to soil structure and mechanical properties. Soil samples are collected from the above tributaries A and B, with sampling sites indicated by red points in Fig. 14, and the cumulative curves for some samples are shown in Fig. 15.

The grain size distribution (GSD) can be described in the following form (Li et al. 2013):

$$P(D) = CD^{-\mu}\exp(-D/D_c), \quad (8)$$

where $P(D)$ is the percentage of grains larger than D (mm); C, μ, and D_c are parameters determined by the frequency data in Fig. 15. As C is associated with μ, the GSD reduces to the two parameters μ and D_c, with μ representing the fine content and D_c is a characteristic grain size representing the grain size range (Li et al. 2013, 2017). GSD parameters for the samples are listed in Table 5.

Soil properties have been found to be well featured by μ and D_c (Gou et al. 2015; Li et al. 2015a, b; Wang et al. 2017). Table 5 indicates that the soils are similar in fine content (featured by μ) while different in coarse grains (featured by D_c). As μ falls into the range between 0.06 and 0.10, the soils by nature are potential to debris flows according to the critical limit of initiation of granular flow (Li et al. 2013). Moreover, the left bank slope has higher content fine grains (μ is 0.094 on average) and wider range of grain size (D_c is 14.98 mm on average) than the right bank slope (μ ~ 0.075 and D_c ~ 7.68 mm on average). Given the moisture conditions, the GSD difference will make great difference in porosity and soil strength (cohesion and friction angle) and cause different behaviors. As indicated by field experiments on slopes with different grain compositions (Guo et al. 2016b), soil failures occur easily and frequently on slope with high value of μ. And experiments of Iverson et al

Table 4 Material distribution in Dawazi Gully

Slopes (°)	15–20	20–25	25–30	30–35	35–40	40–45	45
Area (10^3 m^2)	2.56	33.21	2.87	9.9	94.94	319.75	23.88

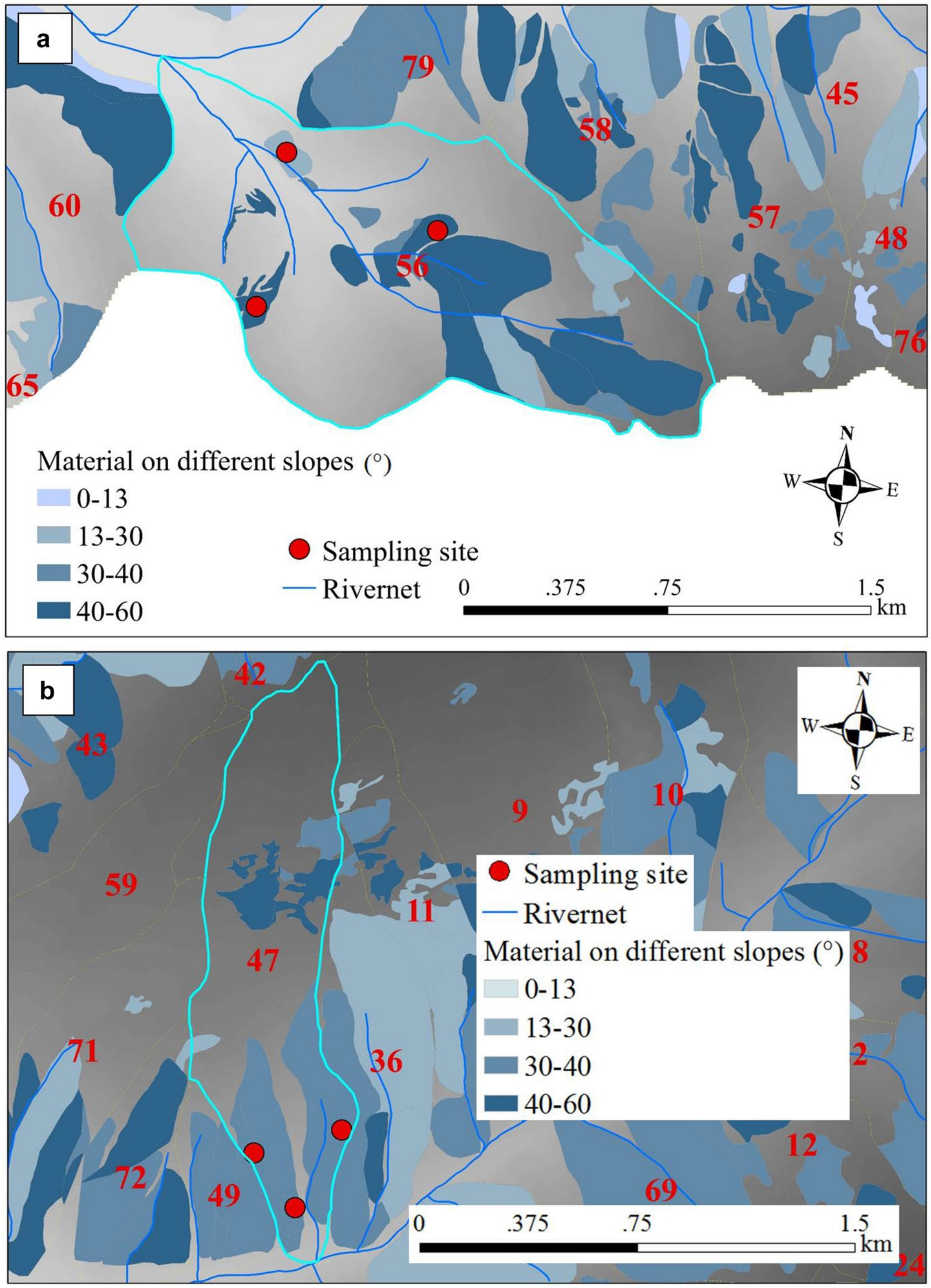

Fig. 14 Material distribution in typical tributaries (**a** an active tributary in Menqian; **b** a stable tributary in the lower reach of JJG)

(2000) indicate that even small difference in initial porosity is enough to result in dramatically different slope processes, such as the imperceptibly slow movement or the catastrophically accelerated motion.

More generally, a soil slope consists of a wide range of grains and each block of material may take different GSD parameters and thus have different physical and mechanical properties associated with a variety of slope processes. According to field surveys in JJG, for a slope or a deposit body, the GSD parameter μ satisfies the Weibull distribution (cf. Eq. 5). Table 6 shows the distribution parameters for flows and deposits.

The Weibull parameters are helpful for distinguishing soil slopes of different potential to debris flows. For example, the soil with λ near the flows are expected to have a higher potentiality because they may turn into flow with less variation of grain composition and thus involve less energy dissipation and momentum transition in the processes from soil to flow. Physically, these processes are always accompanied by infiltration and fine grain migration and the high value

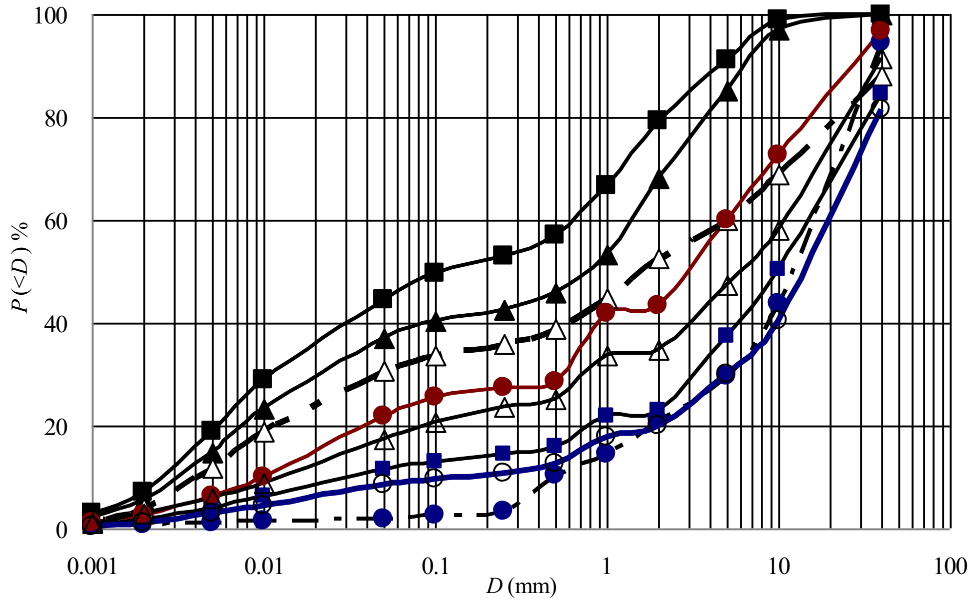

Fig. 15 Frequency distribution of grain size for soil samples

Table 5 GSD parameters of material samples

Tributaries	Sediment deposits		Left bank slope		Right bank slope	
	μ	D_c	μ	D_c	μ	D_c
Lower tributary	0.05	3.38	0.07	8.61	0.07	7.16
	0.07	4.32	0.08	21.16	0.07	7.68
	0.05	3.50	0.07	16.08	0.08	9.69
	0.06	3.26	0.08	14.64	0.08	9.13
	0.07	3.49	0.08	4.56	0.08	7.56
	0.07	6.06	0.10	11.27	0.10	15.01
	0.05	2.55	0.10	18.49		
	0.07	4.07	0.07	8.61		
	0.06	4.03	0.08	21.16		
Tributaries of Menqian	0.08	9.94	0.08	14.28	0.06	3.98
	0.08	7.58	0.10	11.41	0.08	11.25
	0.08	6.98	0.09	12.50	0.10	16.53
	0.08	1.48	0.08	7.35	0.08	6.34
	0.06	5.40	0.11	11.68	0.07	5.24
	0.10	9.75	0.09	8.65	0.08	11.12
	0.08	6.58	0.10	15.49	0.07	5.22
	0.06	4.06	0.10	21.68	0.07	4.99
	0.08	8.11	0.10	17.64	0.07	5.57
			0.09	29.12	0.07	6.55

Table 6 Weibull distribution of GSD parameter for different materials

Materials	Weibull parameters		Samples
	λ	k	
Debris flow fluids	0.097	1.9	205
Debris flow deposits	0.047	1.43	254

of μ on average (hence high λ) always plays an active role (Wang et al. 2017).

In fact, red–yellow soil is dominant in the sources, accounting for 63% of the area, with porosity between 0.41 and 0.51 and infiltration rate up to 0.16 mm/s, which is in favor of loss of fine grains during the seepage of rainfall. Moreover, it is found that the permeability coefficient

Table 7 Stable infiltration rate of various land types

Land types	Stable infiltration rate (mm/s)		
	Red soil	Dawazi Gully	Menqian Gully
Waste land	0.014	–	0.091
Grass land	0.056	–	0.075
Wood land	–	0.072	0.149
Cultivated land	0.079	0.106	0.156
Bare land	0.014	–	–

increases exponentially with μ under given conditions of initial water moisture.

Generally, infiltration varies much with soil, land use, vegetable cover, and season. As shown in Table 7, the infiltration rate is much higher in the Menqian than in the Dawazi and other regions, which provides a favorable condition of water flood in stream channel.

Potential of material in different tributaries

The little differences of material distributions with altitude and aspect indicate that the materials are irrelevant to some single factors (e.g., elevation, temperature and rainfall); but at tributary scale, they present a great variety of appearances. As shown in Fig. 16, photo A is a well-developed tributary channel, B shows slopes in the source of a tributary, and C is a tributary by the mainstream channel, with fragmented slopes in its upper reaches.

Moreover, the fact that debris flows mainly come from some special areas strongly suggests that materials in different tributaries are in different potentiality to debris flows. Although material sources are governed by the tectonic and rock backgrounds, their behaviors depend mainly on local conditions of the tributaries, including landform and rainfall conditions, as well as the connectivity of the tributaries, which influences how the tributary flows converge into the mainstream channel. For illustration, a comparison between the Menqian and Duozhao branches is made in details as follows.

The most remarkable is the difference between the two major branches, the Menqian and Duozhao (Fig. 13): debris flows in the last decades have almost come from Menqian. The difference in debris flow activity cannot be ascribed to the material sources, because both branches are abundant of loose materials, with quantities, respectively, of 5.2×10^8 m^3 and 2.3×10^8 m^3; and the areas of 5.67 km^2 and 4.62 km^2 (cf. Table 1). Neither can this difference be ascribed to the existence of a platform (or mesa) in Duozhao, since this platform only obstructs the local activities but cannot prevent other tributaries from developing debris flows. So, there should be other causes for the absence of debris flow in Duozhao. An obviously possible cause is the connectivity of the materials. In Menqian, one sees huge blocks of materials are concentrated; while in Duozhao, there are only relatively small and scattering material blocks. The concentration of material can be well described by the "area density" defined as the ratio of material area to the tributary area. As indicated by Table 8, the density in Menqian is about a half higher than that in Duozhao.

Another possible cause relies in the structure of tributaries of the two branches: Menqian has a well-developed tree-shape water system constituting tributaries from lower to higher orders; while Duozhao has a braided drainage system with several channels of long stream length. Obviously, the former more easily facilitates the cascading supplies of materials from upper tributaries to the lower. While the latter makes it hard for source materials move down to the lower reaches. This can be featured by the drainage density link length distribution, combining with the distribution of material blocks as the "nodes" at the link ends.

The comparison between Menqian and Duozhao reveals that debris flow depends not only on the material sources but also on the drainage structure. As the geometry of the drainage system is easily understandable, we still focus the materials in Menqian tributaries in the following (Fig. 17).

Discussions: implication of material sources in debris flow occurrence

The material source distribution and properties discussed above provide the material stage of various potentiality for debris flows. As for how the stage plays a role in determining the occurrence of debris flow, it is helpful to consider a real case of debris flow event.

For a specific event, rainfall is the necessary triggering factor. But, in practice, it is hard to associate a debris flow with specific rainfall condition because rainfall in mountainous valley is always non-uniform. In the case of JJG, nine rainfall monitoring stations are placed, considering different local conditions of climate and weather factors (e.g., elevation, aspect, vegetation cover, soil type, land use, and landform) (Fig. 18), and the records of these gauges provide a heterogeneous distribution of rainfall.

Figure 19 shows a rainfall event between 23 and 24, June 2014 recorded by four stations, presenting different intensity, duration, and fluctuation, which are usually taken as crucial indices for predicting of debris flow occurrence (Caine 1980; Guzzetti et al. 2008; Guo et al. 2016a). But in the present situation, rainfall varies much in space and covers different material sources; therefore even under the same rainfall event, it is impossible to determine which rainfall is responsible for the occurrence; moreover, materials in different

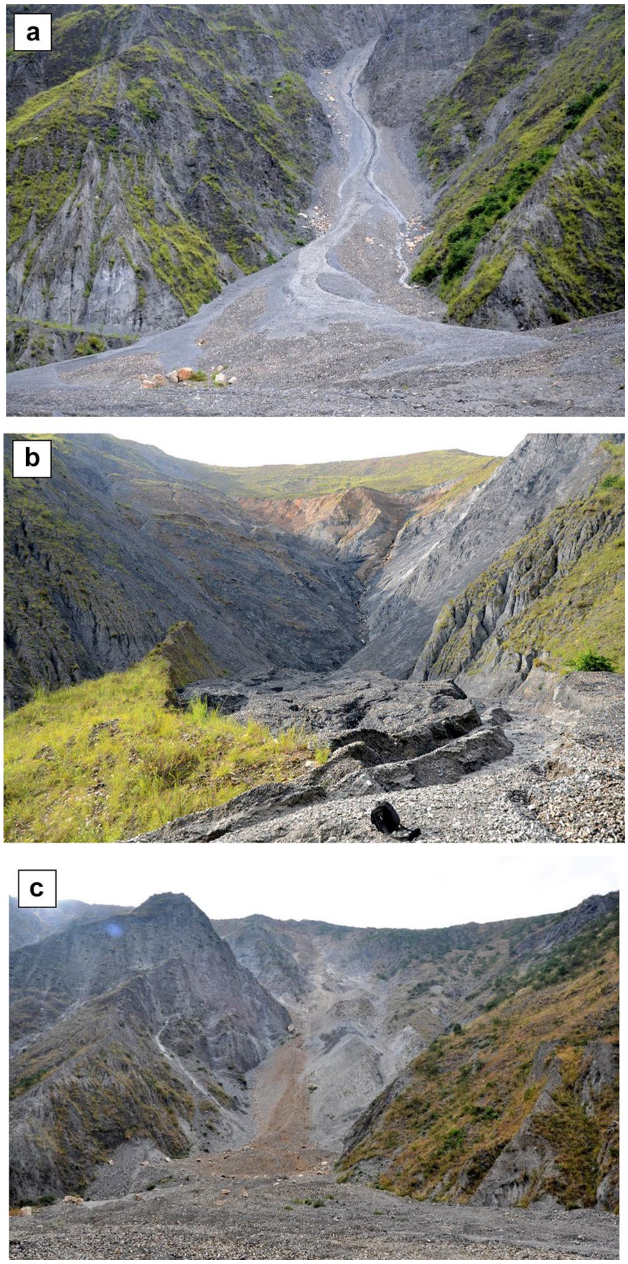

Fig. 16 Materials distribution in different tributaries and slopes

tributaries may respond in different manners. What is practically possible is to construct the forming processes through associating local rainfall with specific material source.

The rainfall record, at first glimpse, suggests that debris flow should have been concentrated between 1:00 and 10:00 on 24 June, when rainfall covered the whole valley and all possible sources might be initiated. But in reality, debris flow (including hyperconcentrated flows) only occurred at 5:25 and ended at about 9:00 on June 24. Especially, the typical debris flows were concentrated only between about 6:00 and 7:00 (Fig. 20). This implies that debris flows do not

Table 8 Material source areas in Menqian and Duozhao Gully in JJG

Subregion	Drainage area (km^2)	Area percentage (%)	Material sources	
			Area (km^2)	Density (%)
Menqian Gully	12.52	27.12	5.67	45.32
Duozhao Gully	15.01	32.52	4.62	30.81

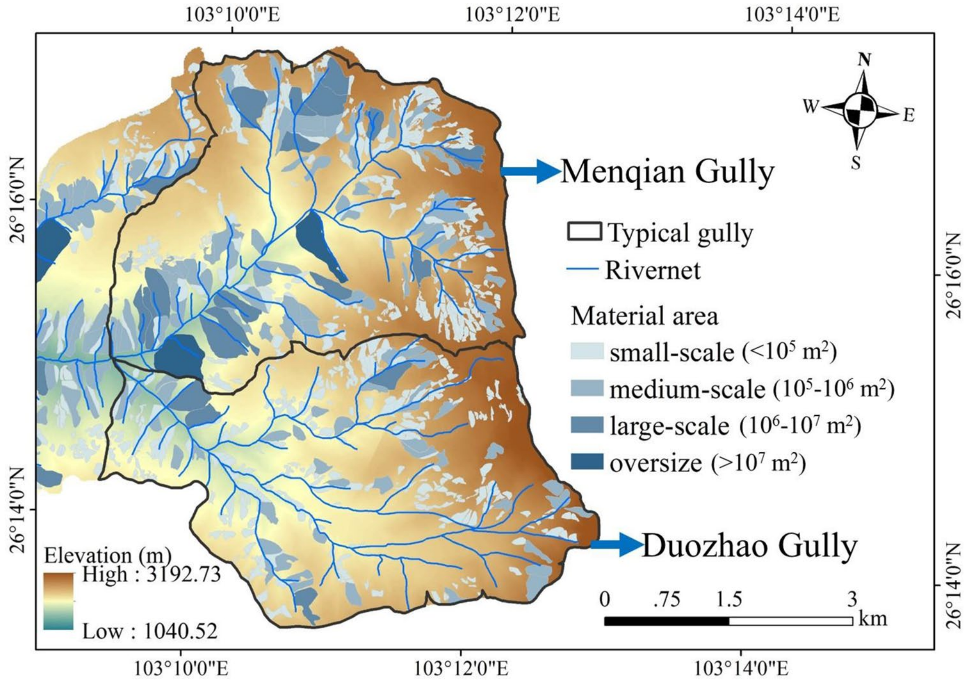

Fig. 17 Material distribution in Menqian and Duozhao

occur simply as responding synchronously to rainfalls and flood flows. Moreover, the discharge fluctuates considerably from about 10 m^3/s to more than 500 m^3/s, and this fluctuation cannot be responding to any variation of the rainfall, because such a rainfall event cannot result in any hydrological processes with fluctuation up to two orders of magnitude.

Indeed, the occurrence and fluctuation of debris flow surges can be traced to the material sources and their response to the local rainfall. Comparing the surge series with the rainfall records, several facts concerning debris flow formation can be inferred:

1. The flows came from the rainfall regions of R6 and R8, in the Menqian;
2. No debris flows occurred in Duozhao even there were heavy rainfalls in R3 region;

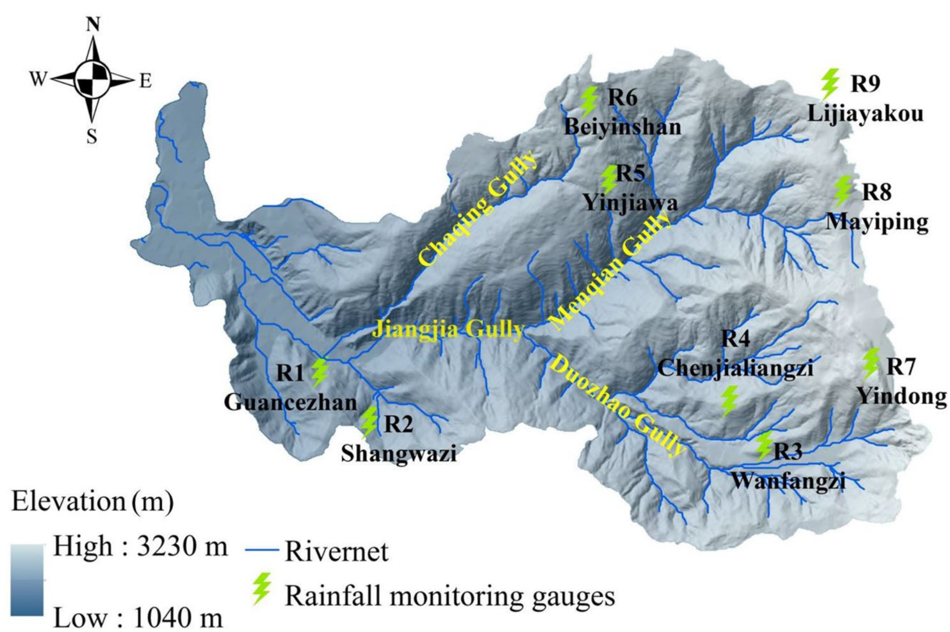

Fig. 18 Rainfall monitoring gauges in JJG

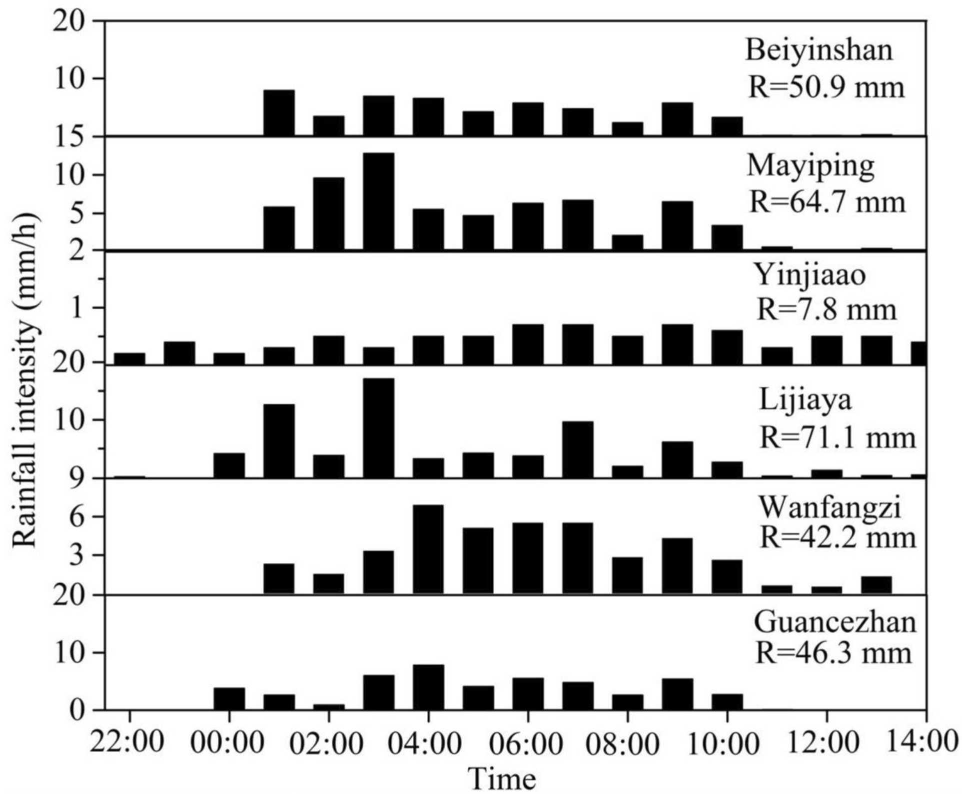

Fig. 19 Rainfall records of different stations on 23–24 June 2014

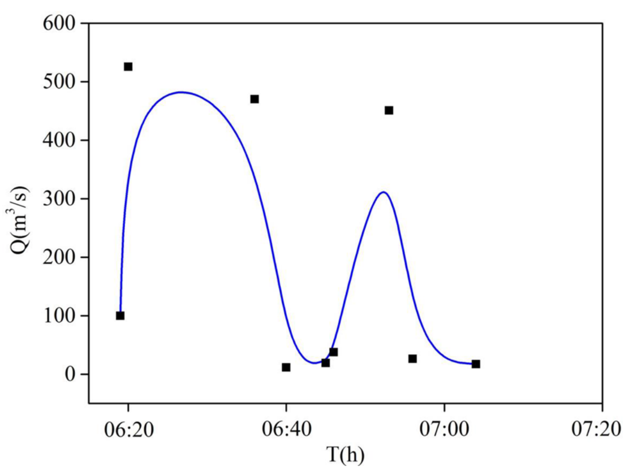

Fig. 20 Debris flow surges on June 24th, 2014

3. Debris flow may occur with a rather long time lag after the rainfall.

In details, all these processes are dependent on the slope processes and water–soil interactions. Rainfall is responsible for changes in soil structure and initiation of failure and flow. Field experiments and observations indicate that both failure size and failure frequency on a slope rise exponentially with rainfall intensity (Guo et al. 2016b).

Generally, debris flow can be considered as such a process that combines the continuous water flows and discontinuous soil supplies. Rainfall governs the water flow process while materials in response to rainfall determine the manners of mass movements (e.g., soil failures, landslides, avalanches, and surface flows). Specifically, the spatial distribution of material sources in various tributaries provides the very stage for the material processes.

Conclusions

A comprehensive investigation of debris flow material sources is conducted in JJG. It is found that most materials are distributed in young tributaries, e.g., with evolution index between 0.55 and 0.65. More important is that debris flow does not rely on the quantity of the material, but on some specific conditions:

1. Materials are concentrated on a localized region, such as the Menqian Gully of JJG, where material blocks are widely distributed on slopes and tributaries near the mainstream;
2. Materials are composed of soils with special granular structure featured by the scaling grain size distribution (GSD) parameters (μ, D_c) falling into a certain value range (e.g., $\mu < 0.1$ in the case study of JJG);

3. Materials are located in regions receiving frequent rainfalls.

Besides the material locations and properties, the occurrence of debris flow also depends strongly on the pattern of drainage system. For example, the high frequency (or absence) of debris flow in Menqian (or Duozhao) is well illustrated by the difference in tributary structure: the tributaries in Menqian form a cascading drainage system which facilitates the developing of debris flows from multiple sources in tributaries of various orders; and tributaries in Duozhao form a braided drainage system with long links, which hampers the flow down to the mainstream channel.

In summary, the problem of debris flow sources should consider both the materials (together with their attributes) and their locations in the watershed system. The material determines the presence or absence of debris flow, while the tributary structure governs the manner of flow developing. It is the spatial heterogeneity of tributary evolution and material source distribution that control the forming and developing of variety of debris flow surges. The present study provides an example illustrating how these aspects are combined together to influence debris flows.

Acknowledgements This study is supported by the Strategic Priority Research Program of the Chinese Academy of Sciences (Grant no. XDA230902) and the Key International S&T Cooperation Projects (Grant no. 2016YFE0122400).

References

Arattano M, Marchi L (2000) Video-derived velocity distribution along a debris flow surge. Phys Chem Earth (B) 25(9):781–784
Blackwelder E (1928) Mudflows as a geologic agent in semiarid mountains. Bull Geol Soc Am 39:465–484
Blahut J, van Westen CJ, Sterlacchini S (2010) Analysis of landslide inventories for accurate prediction of debris-flow source areas. Geomorphology 119:36–51
Broscoe AJ, Thompson S (1969) Observations on an alpine mudflow, Steel Creek, Yukon. Can J Earth Sci 6:219–229
Caine N (1980) The rainfall intensity-duration control of shallow landslides and debris flows. Geografiska Annaler Ser A Phys Geogr 62:23–27
Chen N, Han W, He J, Yan H (2001) Gravity-driven debris flows in a small gully in the northeast Tunnan. Journal of Mountain Science 19(5):418–421 **(In Chinese)**
Chen H, Lee CF (2000) Numerical simulation of debris flows. Can Geotech J 37(1):146–160
Crowley JK, Hubbard BE, Mars JC (2003) Analysis of potential debris flow source areas on Mount Shasta, California, by using airborne and satellite remote sensing data. Remote Sens Environ 87(2):345–358
Cui P, Chen XQ, Wang YY, Hu KH, Li Y (2005) Jiangjia Ravine debris flows in south-western China. In: Jakob M, Hungr O (eds) Debris-flow hazards and related phenomena. Springer, Praxis, pp 565–594
Davies TR, Phillips CJ, Pearce AJ, Zhang XB (1991) New aspects of debris flow behavior. In: Proceedings, U.S.-Japan workshop on snow avalanches, landslides, debris flows prediction and control, Tsukuba, Japan, pp 443–451
Davies TR, Phillips CJ, Pearce AJ, Zhang X (1992) Debris-flow behavior–an integrated overview. In: Proceedings, international symposium on erosion, debris flow and environment in mountain regions, IAHS Publication, Chengdu, China. No. 206, pp 217–226
Dong JJ, Lee CT, Tung YH (2009) The role of the sediment buget in understanding debris flow susceptibility. Earth Surf Process Landforms 34(2):1612–1624
Du RH, Kang ZC, Chen XQ (1987) Investigation and prevention planing of debris flows in Xiaojiang River, Yunnan. Chongqing Branch of Science and Technology Literature Press, Chongqing **(In Chinese)**
Fannin RJ, Wise MP (2001) An empirical-statistical model for debris flow travel distance. Can Geotech J 38:982–994
Garcia-Davalillo J, Herrera G, Notti D, Strozzi T, Alvarez-Fernandez I (2014) DInSAR analysis of ALOS PALSAR images for the assessment of very slow landslides: the Tena valley case study. Landslides 11:225–246
Gonzalez-Diez A, Fernandez-Maroto G, Doughty MW, Diaz de Teran JR, Bruschi V, Cardenal J, Perez JL, Mata E, Delgado J (2014) Development of a methodological approach for the accurate measurement of slope changes due to landslides, using digital photogrammetry. Landslides 11:615–628
Gou WC, Li Y, Wang BL, Liu DC (2015) Grain composition and soil strength of debris flows in Jiahe Gully. Sci Technol Eng 15(35):136–140 **(In Chinese)**
Guo XJ, Cui P, Li Y, Ma L, Ge YG, Mahoney WB (2016a) Intensity-duration threshold of rainfall-triggered debris flows in the Wenchuan Earthquake affected area, China. Geomorphology 253:208–216
Guo XJ, Li Y, Cui P, Zhao WY, Jiang XY, Yan Y (2016b) Discontinuous slope failures and pore-water pressure variation. J Mount Sci 13(1):116–125. https://doi.org/10.1007/s11629-015-3528-4
Guzzetti F, Peruccacci S, Rossi M, Stark C (2008) The rainfall intensity–duration control of shallow landslides and debris flows: an update. Landslides 5:3–17
Iverson RM, Reid ME, Iverson NR, LaHusen RG, Logan M, Mann JE, Brien DL (2000) Acute sensitivity of landslide rates to initial soil porosity. Science 290:513–516. https://doi.org/10.1126/science.290.5491.513
Iverson RM (2014) Debris flows: behavior and hazard assessment. Geol Today 30(1):15–20
Iverson RM, George DL (2016) Modelling landslide liquefaction, mobility bifurcation and the dynamics of the 2014 Oso disaster. Geotechnique 66:175–187
Kappes MS, Malet JP, Remaitre A, Horton P, Jaboyedoff M, Bell R (2011) Assessment of debris-flow susceptibility at medium-scale in the Barcelonnette Basin. France Nat Hazards Earth Syst Sci 11:627–641
Li Y, Liu JJ, Hu KH, Su PC (2012) Probability distribution of measured debris-flow velocity in Jiangjia Gully, Yunnan Province, China. Nat Hazards 60(2):689–701
Li Y, Liu J, Su F, Xie J, Wang B (2015a) Relationship between grain composition and debris flow characteristics: a case study of the Jiangjia Gully in China. Landslides 12:19–28. https://doi.org/10.1007/s10346-014-0475-z
Li Y, Wang BL, Zhou XJ, Gou WC (2015b) Variation in grain size distribution in debris flow. J Mount Sci 12:682–688. https://doi.org/10.1007/s11629-014-3351-3
Li Y, Zhou X, Su P, Kong Y, Liu J (2013) A scaling distribution for grain composition of debris flow. Geomorphology 192:30–42. https://doi.org/10.1016/j.geomorph.2013.03.015
Li J, Luo DF (1981) The formation and characteristics of mudflow and flood in the mountain area of the Daqiao River and its prevention. Z Geomorph N F 25(4):470–484

Li J, Yuan J, Yuan JM, Bi C, Luo DF (1983) The main features of the mudflow in Jiangjia Ravine. Z Geomorph N F 27(3):325–341
Li Y, Yue ZQ, Lee CF, Beighley RE, Chen X-Q, Hu K-H, Cui P (2009) Hack's law of debris-flow basins. Int J Sediment Res 24:74–87. https://doi.org/10.1016/S1001-6279(09)60017-2
Li Y, Hu K, Yue ZQ, Tham TG (2004) Termination and deposition of debris-flow surge. In: Lacerda W, Ehrlich M, Fontoura SA, Sayao AS (Eds) Landslides: evaluation and stabilization. 2004 Taylor & Francis Group, London, pp 1451–1456
Limerinos J (1970) Determination of the manning coefficient from measured bed roughness in natural channels. Technical report, USGS Water Supply Paper 1898-B
Lorente A, Begueria S, Bathurst JC, Garcia-Ruiz JM (2003) Debris flow characteristics and relationships in the Central Spanish Pyrenees. Nat Hazards Earth Syst Sci 3:683–691
Major JJ (1997) Depositional processes in large-scale debris-flow experiments. J Geol 105:345–366
Monin AS, Yaglom AM (1975) Statistical fluid mechanics, vol 2. MIT Press, Cambridge Mass
Nakata AM, Matsushima T (2014) Landslide simulation based on particle method: toward statistical risk evaluation. COMPSAFE2014, pp 397–399
Pierson TC (1980) Erosion and deposition by debris flows at Mt. Thomas, North Canterbury. N Z Earth Surf Process 5:227–247
Pierson TC (1986) Flow behavior of channelized debris flowss, Mount St. Helens, Washington. In: Abrahams AD (ed) Hillslope Processes (The Binghamton Symposia in Geomorphology: International Series, No. 16), Allen and Unwin, Inc., pp 269–296
Qiao JP, Huang D, Yang ZJ, Meng HJ (2012) Statistical method on dynamic reserve of debris flows source materials in meizoseismal area of Wenchuan earthquake region. Chin J Geol Hazard Control 23(2):1–6 **(in Chinese)**
Rickenmann D (1999) Empirical relationships for debris flows. Nat Hazards 19:47–77
Rickenmann D, Laigle D, Mcardell BW, Hubl J (2006) Comparison of 2D debris-flow simulation models with field events. Comput Geosci 10:241–264
Rickmers WR (1927) The duab of turkestan. Cambridge University Press, Cambridge
Royan MJ, Abellan A, Jaboyedoff M, Vilaplana JM, Calvet J (2014) Spatio-temporal analysis of rockfall pre-failure deformation using Terrestrial LiDAR. Landslides 11:697–709
Santi PM, Dewolfe VG, Higgins JD, Cannon SH, Gartner JE (2008) Sources of debris flow material in burned areas. Geomorphology 96(3–4):310–321
Sharp RP (1953) Mudflow of 1941 at Wrightwood, southern California. Geol Soc Am Bull 64:547–560
Sharp RP (1942) Soil structures in the St. Elias Range, Yukon Territory. J Geomorphol 5:274–301
Shieh CL, Jan CD, Tsai YF (1996) A numerical simulation of debris flow and its application. Nat Hazards 13:39–54
Strahler AN (1952) Hypsomic analysis of erosional topography. Bull Geol Soc Am 63:1117–1142
Strahler AN (1957) Quantitative analysis of watershed geomorphology. Eos Trans Am Geophys Union 38:913–920
Takahashi T (2007) Debris flow mechanics, Prediction and Countermeasures. Taylor & Francis/Balkema, Milton Park
Takahashi T (1991) Debris flow. IAHR/AIRH Monography Series. A. A Balkeman, Rotterdam
Tian LQ (1987) Geomorphology and debris flow of Jiangjia Gully. J Mount Sci 5(4):203–212 **(In Chinese)**
Tunusluoglu MC, Gokceoglu AC, Nefeslioglu AHA, Sonmez AH (2008) Extraction of potential debris source areas by logistic regression technique: a case study from Barla, Besparmak and Kapi mountains (NWTaurids, Turkey). Environ Geol 54:9–22
Wang B, Li Y, Gou W, Guo C, Yao L (2017) Fine grain migration and its impact on soil failures under rainfall infiltration. Adv Eng Sci 49(Supp. 2):40–50 **(In Chinese)**
Wu JS, Kang ZC, Tian LQ (1990) Observation and study of debris flows in Jiangjia Gully, Yunnan. Science Press, Beijing **(in Chinese)**
Yang RW (1997) Solid material supplied volume to debris flow in Jiangjia ravine, Yunnan province. J Mount Res 15(4):305–307